Diagnostic performance of fast brain MRI compared to routine clinical MRI in patients with glioma grade 3 and 4 - a pilot study

Francesca De Luca, Annika Suneson, Annika Kits, Emilia Palmér, Stefan Skare, Anna Falk Delgado

ABSTRACT

BACKGROUND AND PURPOSE: EPIMix is a fast brain MRI technique not previously investigated in patients with glioma grades 3 and 4. This pilot study aimed to investigate the diagnostic performance of EPIMix in the radiological treatment evaluation of adult patients with glioma grades 3 and 4 compared to routine clinical MRI (rcMRI).

MATERIALS AND METHODS: Patients with glioma grades 3 and 4 investigated with rcMRI and EPIMix were retrospectively included in the study. Three readers (R1–3) participated in the radiological assessment applying Response Assessment for Neuro-oncology Criteria (RANO 2.0), of which two (R1–2) independently evaluated EPIMix and later rcMRI by measuring contrast-enhancing and non-contrast-enhancing tumor regions at each follow-up. For cases with discrepant evaluations, an unblinded side-by-side (EPIMix and rcMRI) reading was performed together with a third reader (R3). Comparisons between methods (EPIMix vs. rcMRI) were performed using Weighted Cohen's kappa. The sensitivity and specificity to detect tumor progression (PD) on a follow-up scan were calculated for EPIMix compared to rcMRI with receiver operating characteristic (ROC) curves to assess the area under the curve (AUC).

RESULTS: In 35 patients (mean age 53, 31 % females), a total of 93 MRIs encompassing 58 follow-up investigations showed PD at blinded reading in 33% of EPIMix (19/58, R1–2), while in 31% (18/58 exams, R1), and 34% (20/58 exams, R2) of rcMRI. An almost perfect agreement for tumor category assessment was found between EPIMix and rcMRI (EPIMixR1 vs. rcMRIR1 $\varkappa$= 0.96; EPIMixR2 vs. rcMRIR2 $\varkappa$= 0.89). The sensitivity for EPIMix to detect PD was 1.00 (0.81–1.00) for R1 and 0.90 (0.68–0.99) for R2, while the specificity was 0.97 (0.86–1.00) for R1–2. The AUC for PD was 0.99 for R1 (EPIMixR1 vs. rcMRIR1) and 0.94 for R2 (EPIMixR2 vs. rcMRIR2), DeLong's test AUCR1 vs. AUCR2 p=0.20 (R1–2).

CONCLUSIONS: In this pilot study, EPIMix was used as a fast MRI alternative for treatment evaluation of patients with glioma grades 3 and 4, with high, but slightly lower diagnostic performance than rcMRI.

ABBREVIATIONS: CR = complete response; EPIMix = multi-contrast echo-planar imaging-based technique; PD = progressive disease; PR = partial response; RANO = response assessment in neuro-oncology; R1 = reader 1; R2 = reader 2; R3 = reader 3; rcMRI = routine clinical MRI; SD = stable disease.

Received month day, year; accepted after revision month day, year.
From the Department of Radiology, Karolinska University Hospital, Stockholm, Sweden (FDL); Department of Neuroradiology, Karolinska University Hospital, Stockholm, Sweden (AS, AK, SS, AFD); Department of Medical Radiation Physics and Nuclear Medicine, Karolinska University Hospital, Stockholm, Sweden (EP); Department of Clinical Neuroscience, Karolinska Institutet, Stockholm, Sweden (FDL, AK, SS, AFD); Department of Molecular Medicine and Surgery, Karolinska Institute, Stockholm, Sweden (EP).

The authors declare no conflicts of interest related to the content of this article.

Please address correspondence to Francesca De Luca, MD, Department of Radiology, Karolinska University Hospital, Department of Clinical Neuroscience, Karolinska Institutet, Stockholm, 17176, Sweden; francesca.de.luca@ki.se

SUMMARY SECTION

PREVIOUS LITERATURE: The multi-contrast echo-planar imaging-based technique EPIMix includes five 2D MRI sequences (T1, T2, T2-FLAIR, DWI/ADC, and T2*-weighted images) with high relevance for brain imaging. The clinical feasibility of EPIMix has been previously investigated in patients with a broad spectrum of cerebral pathology, with suspicion of acute ischemic stroke, pediatric patients, and evaluation of the image quality of the technique with a proven high diagnostic performance and sufficient image quality. Still, EPIMix has yet to be evaluated in the radiological treatment evaluation of adult patients with glioma grades 3 and 4.

KEY FINDINGS: EPIMix showed high, but slightly lower diagnostic performance than rcMRI in the radiological treatment evaluation of adult patients with glioma grades 3 and 4.

KNOWLEDGE ADVANCEMENT: In this pilot study, EPIMix was used as a fast MRI alternative for treatment evaluation of patients with glioma grades 3 and 4.

INTRODUCTION

Glioma grades 3 and 4 are a heterogeneous group of central nervous system (CNS) tumors with infiltrative growth patterns resembling glial cells at histology (1). In a recent report, grade 3 astrocytoma and grade 4 glioblastoma constituted the predominant histological

subtypes, accounting for 61% of malignant CNS tumors in the US population (2). Patients with glioma grades 3 and 4 routinely undergo frequent, longitudinal radiological follow-ups. In this patient group, MRI is usually preferred over CT due to its high ability to depict high-grade glioma characteristics, such as precise tumor localization, infiltrative growth pattern, and perifocal tumor edema (3). Further, it allows for assessing tumor heterogeneity by visualizing solid and necrotic tumor components as contrast-enhancing areas with central non-contrast-enhancing necrosis.

Routine clinical MRI (rcMRI) examinations in patients treated for glioma grades 3 or 4 include a minimum of pre- and post-contrast T1-weighted, and T2-weighted images (4, 5). However, in a clinical situation, additional sequences are often added, such as diffusion-weighted imaging (DWI) and T2* – or susceptibility-weighted images, with protocols extending up to > 30 minutes (5, 6). Moreover, high spatial image resolution, allowing for multiplanar reconstruction, further extends imaging time compared to non-3D acquisitions (3-5).

In patients with glioma grades 3 and 4, neurological deterioration with reduced compliance to undergo an investigation may hamper imaging. In addition, long brain rcMRI protocols can increase motion artifacts and, thus, lower image quality. Further, lengthy scan times plus limited MRI resources can result in long health queues for patients planned to undergo an MRI exam.

A recently developed multi-contrast echo-planar imaging-based technique (EPIMix) at Karolinska University Hospital provides a complete brain investigation with multiple MRI sequences at a total scan time of 78 seconds (7). Specifically, EPIMix includes five clinically important 2D MRI sequences with high relevance for brain tumor imaging: T1, T2, T2-FLAIR, DWI/ADC, and T2*-weighted images. Similarly to many other existing clinical MRI techniques, EPIMix provides weighted images, not parametric ones like those generated with MRI fingerprinting (8) or synthetic MRI (9). EPIMix is an inherently motion-robust technique with 2D capability that prevents motion artifacts from propagating throughout the entire head volume.

The clinical feasibility of EPIMix has been previously investigated in patients with a broad spectrum of cerebral pathology (10), including suspicion of acute ischemic stroke (11, 12), pediatric patients (13), but has yet to be evaluated in adult patients with glioma grades 3 and 4. EPIMix might benefit patients with brain tumors since it allows for a brain investigation at a markedly shorter scan time, thus limiting the possibility of patient discomfort and motion artifacts, possibly reducing waiting queues for MRI. It might also be an alternative for patients with claustrophobia by limiting time in enclosed spaces. Thus, this study aimed to evaluate the diagnostic performance of EPIMix compared to rcMRI in the radiological follow-up of patients with glioma grades 3 and 4.

MATERIALS AND METHODS

This retrospective pilot study was designed and reported according to the diagnostic accuracy STARD guidelines (14), see Supplementary Table 1.

Participants

Patients with ≥ two postoperative rcMRI scans and simultaneously acquired EPIMix investigated at the Medical Department of Neuroradiology, Karolinska University Hospital, between July 2017 and May 2020 were retrospectively included in this study. Inclusion criteria were patients with pathologically confirmed glioma grades 3 or 4, ≥ 18 years old at image acquisition. Exclusion criteria were: lack of histological confirmation, nonavailability of the post-contrast T1-weighted sequences, less than two postoperative EPIMix and rcMRI, or substantial image artifacts on both EPIMix and rcMRI rendering images uninterpretable. The co-existence of other brain

pathologies did not lead to exclusion. Clinical information and pathological reports were obtained by reviewing referrals and medical charts. The study was approved by the regional Swedish Ethical Review Authority, which waived the need for informed consent due to the retrospective nature of the study (approval number/ID 2019-01309).

Patients' search strategy

Patients were retrospectively included from the local Radiology Information System (RIS) at Karolinska University Hospital using search criteria defined in MAMP (https://www.mamp.info/en/mac/) with MySQL query language (available online at https://dev.mysql.com/doc/relnotes/mysql/8.0/en/news-8-0-20.html). Terms were combined and truncated as appropriate (Supplementary Text 1). Manual screening of eligible patients in the Picture Archiving and Communication System (PACS) was performed to ensure a correct application of the exclusion criteria.

Image acquisition

EPIMix and rcMRI were acquired on a GE SIGNA Premier 1.5T and 3T (GE Healthcare, Milwaukee, WI) MRI system.

EPIMix

EPIMix is a 2D echo-planar imaging-based MRI technique including five axial sequences (T1-FLAIR, T2, T2-FLAIR, DWI/ADC, T2*) with 4 mm slice thickness, 240 mm FOV, 180×180 matrix, and an acceleration factor of R=3, at a total scan time of 78 seconds. At our institution, EPIMix has been added as a motion-robust addition to the routine clinical sequences to achieve contrast redundancy when artifacts corrupting rcMRI were expected. Detailed information about the EPIMix technique has been published previously by Skare et al. (7)

rcMRI

Imaging sequences included T1, T2, T2-FLAIR, DWI/ADC, T2*, and/or SWI (93 out of 93 MRI scans, Figure 1) and perfusion-weighted images (36 out of 93 MRI scans). Supplementary Table 2 provides detailed information on the rcMRI scan protocols developed in accordance with the consensus recommendations for a standardized brain tumor imaging protocol (5).

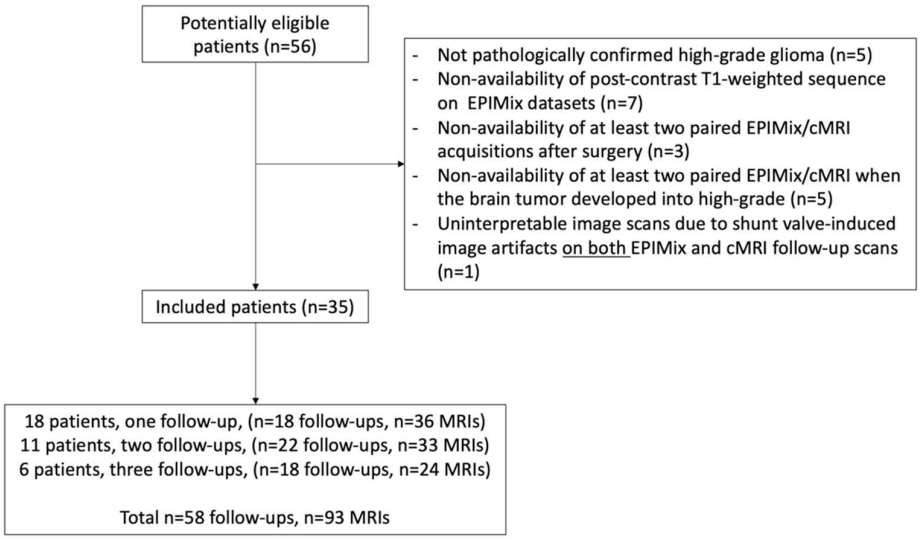

FIG 1. A flowchart of included patients and MRI scan evaluations.

Radiological assessment

Three readers participated in the image evaluation (R1–3). Initially, two blinded readers independently evaluated EPIMix and rcMRI on separate occasions: reader one (R1) – a radiology resident with two years of radiology experience – and reader 2 (R2) – a neuroradiologist with seven years of neuroradiology experience. To avoid recall bias favoring the new method, EPIMix was analyzed first, followed by a memory washout period of at least two weeks before reading rcMRI. For both methods, pre- and post-contrast T1-weighted were evaluated. In one case, due to the unavailability of pre-contrast EPIMix series, post-contrast T2*-weighted EPIMix was used for comparison with the post-contrast T1-weighted EPIMix image to discriminate blood products from contrast-enhancement. The readers were blinded to all clinical information, including health records, referral information, and radiology reports. The first available postoperative MRI with paired EPIMix and rcMRI served as the baseline for comparison with subsequent follow-up scans. Tumor measurements were obtained on baseline and follow-up scans according to predefined radiological criteria adapted from the Response Assessment for Neuro-Oncology criteria (RANO 2.0) for contrast-enhancing gliomas (15), see Table 1 and Supplementary Text 2. Follow-up scans were categorized into four predefined radiological tumor status categories: complete response (CR), partial response (PR), stable disease (SD), and progressive disease (PD), Table 1. For cases with discrepant evaluations between readers (EPIMixR1 vs. EPIMixR2; rcMRIR1 vs. rcMRIR2) or between methods (EPIMixR1 vs. rcMRIR1; EPIMixR2 vs. rcMRIR2), an unblinded side-by-side (EPIMix and rcMRI) reading was performed together with a third reader (R3, ten years of neuroradiology experience). This additional review served to clarify potential sources of discrepancies between EPIMix and rcMRI at blinded reading and was thus hypothesis-generating.

Table 1: Radiological tumor status categories used at the blinded reading of EPIMix and rcMRI, modified from (15)

Radiological tumor status categories	
Complete response (CR)	All of the following: • complete disappearance of all enhancing measurable, nonmeasurable disease • no new measurable lesions.
Partial response (PR)	All of the following: • ≥50% decrease in the sum of products of perpendicular diameters of all measurable enhancing target lesions • no new measurable lesions • no progression of nonmeasurable enhancing disease[a]
Stable disease (SD)	All of the following: • stable area(s) of enhancing lesions on imaging • no new measurable lesions • no progression of nonmeasurable enhancing disease[a]
Progressive disease (PD)	At least one of the following: • ≥25% increase in the sum of the products of perpendicular diameters • appearance of a new measurable lesion. In the case where the baseline or best response demonstrates no measurable enhancing disease (visible or not visible), then any new measurable (≥10mm x 10mm) enhancing lesions are considered PD • clear progression of nonmeasurable lesions (increase in bidirectional diameters by at least 5mm x 5mm to ≥10mm x 10mm[a])

The smallest tumor measurement at either baseline or follow-up scans was used for comparison.
The best possible tumor status category at follow-up for patients with nonmeasurable disease only at baseline or no contrast-enhancing lesions at baseline was SD.
[a]Progression of nonmeasurable lesions requires an increase in bidirectional diameters by at least 5mmx5mm to ≥10mmx10 mm. This should be added to the sum of the target lesions. The designation of overall progression requires ≥25% increase in the sum of products of perpendicular diameters.

rcMRI parameter analysis

The contrast-to-noise ratio (CNR) and signal-to-noise ratio (SNR) were calculated for EPIMix and rcMRI using pre-contrast T1-weighted images. Three pairs of regions of interest (ROIs) were delineated in each hemisphere semi-automatically using an in-house code built in MATLAB (R2022b, Mathworks Inc., Natick, MA, USA): one in the caudate nucleus of each hemisphere, one in the white matter of the centrum semiovale of each hemisphere, and one outside the skull, serving as a background reference. The CNR was determined using the formula $CNR = (S1 - S2)/\sigma_N$ (16). Signal intensities were calculated as the average ((right + left)/2) of the mean pixel intensity in the caudate nucleus (S1) and centrum semiovale (S2), respectively. Noise σ_N was calculated as the average ((right + left)/2) of the standard deviation (σ) of the signal intensity in the background ROIs. The SNR was calculated using the average of the mean pixel intensity in the caudate nucleus (S1) and the average of the standard deviation (σ) of background noise (σ_N), according to the formula $SNR = S1/\sigma_N$. In images displaying pathological changes in the caudate nucleus and/or centrum semiovale of one hemisphere, CNR and SNR were calculated using only the ROIs from the contralateral, non-pathological hemisphere. Additionally, ghosting image artifacts were evaluated for EPIMix and rcMRI on pre-contrast T1-weighted images (https://www.acraccreditation.org/-/media/ACRAccreditation/Documents/MRI/LargePhantomGuidance.pdf). Five ROIs were delineated semi-automatically using an in-house code built in MATLAB (R2022b). The ghosting image artifact ratio (R) was calculated using the formula $R = |(B_{top} + B_{btm}) - (B_l + B_r)|/(2 \cdot C)$, where four background ROIs were positioned at the top (B_{top}), bottom (B_{btm}), left (B_l), and right (B_r) of the image, and one ROI was placed at the center within the skull (C).

Statistical analysis

EPIMix assessments were compared against those from rcMRI. Tumor status categories were summarized in separate 4×4 contingency tables (CR, PR, SD, PD) for EPIMix and rcMRI, respectively. Weighted Cohen's kappa (17) was used to evaluate what we refer to as the intra- and inter-reader agreement (Supplementary Table 3 provides Weighted Cohen's kappa interpretation scale). "Intrareader" agreement analysis was defined as EPIMixR1 vs. rcMRIR1 and EPIMixR2 vs. rcMRIR2, while "interreader" agreement analysis was defined as EPIMixR1 vs. EPIMixR2 and rcMRIR1 vs. rcMRIR2. McNemar-Bowker test (18) and Stuart Maxwell test (19) were used to evaluate the symmetry and homogeneity of changes in assessments across tumor status categories between EPIMix and rcMRI (EPIMixR1 vs. rcMRIR1, EPIMixR2 vs. rcMRIR2) and between blinded readers (EPIMixR1 vs. EPIMixR2, rcMRIR1 vs. rcMRIR2). In addition, EPIMix and rcMRI assessments were categorized as follows:

- PD = progressive disease
- SD+PR+CR = nonPD

Categorization into PD and nonPD was performed to compare the diagnostic accuracy of EPIMix to detect PD compared to rcMRI (EPIMixR1 vs. rcMRIR1, EPIMixR2 vs. rcMRIR2) and summarized in a 2×2 contingency table for EPIMix against rcMRI (R1, R2). The receiver operating characteristic curve (ROC) analysis (20) estimated the area under the ROC curve (AUC, 95%CI) for EPIMix against rcMRI (EPIMixR1 vs. rcMRIR1 and EPIMixR2 vs. rcMRIR2). DeLong's test (21) was used to perform pairwise comparisons of ROC curves between blinded readers (AUC R1 vs. AUC R2). The sensitivity and specificity (95%CI) of EPIMix against rcMRI were also calculated. Wilcoxon matched-pairs signed rank test (22) was used to compare SNR and CNR between EPIMix and rcMRI. Statistical analysis was performed using GraphPad Prism (version 10.2.1, GraphPad Software, Boston, Massachusetts USA, www.graphpad.com, San Diego, California USA) and R version 4.4.1 (R Core Team (2024). _R: A Language and Environment for

Statistical Computing_. R Foundation for Statistical Computing, Vienna, Austria. https://www.R-project.org/, packages "irr" version 0.84.1, "vcd" version 1.4-12, "pROC" version 1.18.5, "epiR" version 2.0.75, "DescTools" version 0.99.56).

RESULTS

Study population

Out of 56 potentially eligible patients, 21 were excluded, Figure 1. In 35 included patients (mean age 53, 31 % females), a total of 93 MRIs encompassing 58 follow-up investigations were retrospectively included. Detailed information about patients' characteristics can be found in Table 2. Post-contrast EPIMix was acquired after post-contrast rcMRI in most of the investigations (83/93, 89%). All EPIMix and rcMRI examinations were performed without general anesthesia.

Table 2: Patients' characteristics.

Study participants, n 35	
Age years mean (SD)	53 (14)
Sex female, n (%)	11 (31)
Glioma type and grade* n (%)	
Anaplastic astrocytoma, grade 3, no co-deletion 1p/19q	5 (14)
IDH 1 mutant	3 (60)
IDH 1-2 wildtype	2 (40)
Anaplastic pleomorphic xanthoastrocytoma, IDH 1-2 wildtype, grade 3	1 (3)
Glioblastoma, IDH 1-2 wildtype, grade 4	25 (71)
Anaplastic oligodendroglioma, grade 3, co-deletion 1p/19q	3 (9)
IDH 1 mutant	2 (67)
IDH 2 mutant	1 (33)
Anaplastic ependymoma, IDH 1-2 wildtype, grade 3	1 (3)
Tumor location, n (%)	
Supratentorial only	33 (94)
Supratentorial and infratentorial	2 (6)
Surgery prior to first included paired EPIMix/MRI exam, n (%)	
Resection	29 (83)
Biopsy	6 (17)
Time delay between post-contrast EPIMix and post-contrast rcMRI, minutes mean (range)	
EPIMix prior to rcMRI (n = 10)	3 (1-5)
rcMRI prior EPIMix (n = 83)	6 (3-14)

*According to WHO 2016 classification (23); SD= standard deviation

Longitudinal radiological follow-up

At the blinded reading, EPIMix evaluation detected 33% (19/58, R1–2) of follow-up scans classified as PD, while rcMRI evaluation detected 31% (18/58, R1) and 34% (20/58, R2) of PD. A contingency table of tumor status categories (CR, PR, SD, PD) assessed by blinded readers can be found in Table 3 (EPIMixR1 vs. rcMRIR1, EPIMixR2 vs. rcMRIR2, EPIMixR1 vs. EPIMixR2, rcMRIR1 vs. rcMRIR2). A contingency table of tumor status categories as PD and nonPD assessed by blinded readers can be found in Table 4 (EPIMixR1 vs. rcMRIR1, EPIMixR2 vs. rcMRIR2). The agreement between methods EPIMix and rcMRI (intrareader EPIMixR1 vs. rcMRIR1, EPIMixR2 vs. rcMRIR2) was almost perfect for R1 and R2. No evidence of a difference was found between methods with the McNemar-Bowker test (p=0.80–0.95) and the Stuart Maxwell test (p=0.61–0.85). The agreement between readers R1 and R2 (interreader) was almost perfect for EPIMix (EPIMixR1 vs. EPIMixR2) and rcMRI (rcMRIR1 vs. rcMRIR2), Table 5. No evidence of a difference was found between readers with the McNemar-Bowker test (p=0.39–0.80) and the Stuart Maxwell test (p=0.22–0.61). The sensitivity for EPIMix compared to rcMRI to detect PD was 1.00 (0.81–1.00) in R1 and 0.90 (0.68–0.99) in R2, while the specificity was 0.97 (0.86–1.00) for R1–2, Figure 2. The AUC of EPIMix compared to rcMRI was 0.99 for R1 (EPIMixR1 vs. rcMRIR1) and 0.94 for

R2 (EPIMixR2 vs. rcMRIR2), Table 5, DeLong's test AUCR1 vs. AUCR2 p= 0.20. Detailed results for sensitivity, specificity, ROC analysis, and Weighted Cohen's kappa can be found in Table 5.

Table 3: 4×4 contingency table of tumor status categories assessed by blinded readers (EPIMix vs. rcMRI, EPIMix R1 vs. R2 and rcMRI R1 vs. R2).

	rcMRI R1	CR	PR	SD	PD
EPIMix R1					
CR		**0**			
PR			**2**		
SD				**37**	
PD				**1**	**18**

	rcMRI R2	CR	PR	SD	PD
EPIMix R2					
CR		**0**			
PR			**3**		
SD				**34**	**2**
PD				**1**	**18**

	EPIMix R2	CR	PR	SD	PD
EPIMix R1					
CR		**0**			
PR			**2**		
SD			**1**	**36**	
PD					**19**

	rcMRI R2	CR	PR	SD	PD
rcMRI R1					
CR		**0**			
PR			**2**		
SD			**1**	**35**	**2**
PD					**18**

Table 4: 2×2 contingency table for PD and nonPD categorization on an intrareader basis (EPIMix vs. rcMRI).

	rcMRI R1				**rcMRI R2**		
EPIMix R1		nonPD	PD	**EPIMix R2**		nonPD	PD
	nonPD	39	0		nonPD	37	2
	PD	1	18		PD	1	18

Table 5: Sensitivity, specificity, ROC analysis, and Weighted Cohen's kappa.

	rcMRI R1	TP	TN	FP	FN	Sensitivity (95%CI)	Specificity (95%CI)	AUC (95%CI)
EPIMix R1		18	39	1	0	1.00 (0.81-1.00)	0.97 (0.87-1.00)	0.99 (0.96-1.00)
	rcMRI R2	TP	TN	FP	FN	Sensitivity (95%CI)	Specificity (95%CI)	AUC (95%CI)
EPIMix R2		18	37	1	2	0.90 (0.68-0.99)	0.97 (0.86-1.00)	0.94 (0.86-1.00)

AUC= area under the curve; CI= confidence interval; FN= false-negative; FP= false-positive; R1= reader 1; R2= reader 2; rcMRI= routine clinical MRI; TN= true negative; TP= true positive

	Weighted Cohen's κ
Intrarreader R1-2	
EPIMix R1 vs. rcMRI R1	0.96
EPIMix R2 vs. rcMRI R2	0.89
Interreader R1 vs. R2	
EPIMix R1 vs. EPIMix R2	0.98
rcMRI R1 vs. rcMRI R2	0.91

A p-value <.001 was found for all kappa results in the table.

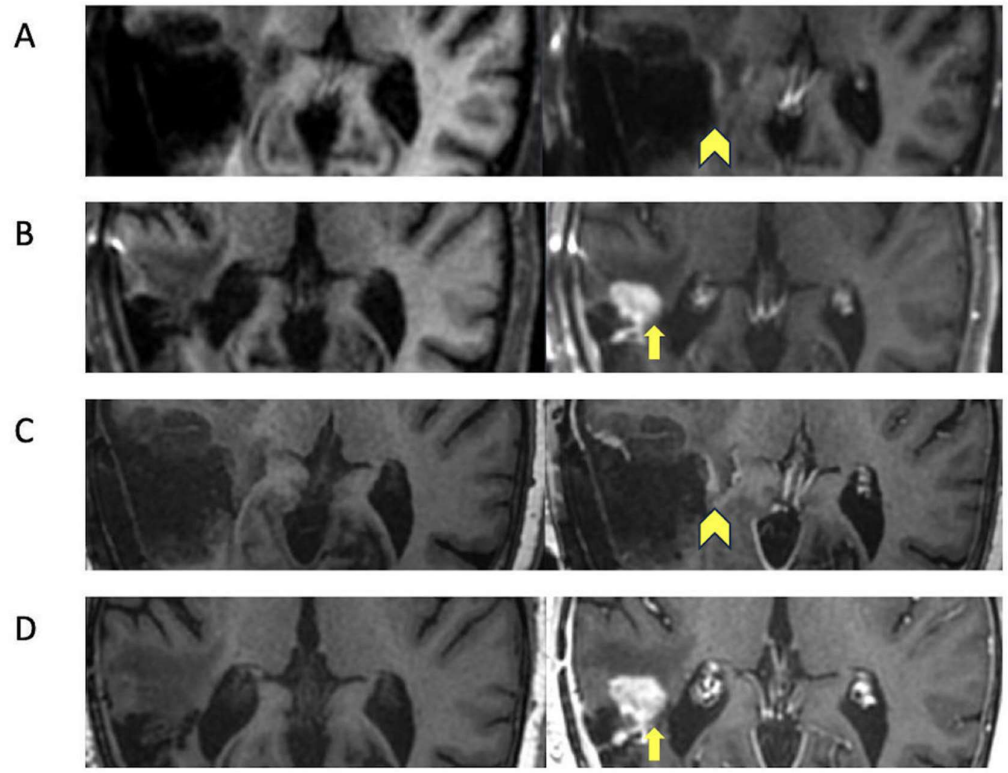

FIG 2. One concordant case where EPIMix shows exact agreement with rcMRI regarding progressive disease at blinded reading. T1-, T1 post-contrast images. A and B, EPIMix baseline and follow-up; C and D, rcMRI baseline and follow-up. Progression from non-measurable (arrowhead) to measurable contrast-enhancing (arrow) lesion is visible on EPIMix follow-up. The contrast-enhancing lesions are just as visible on the corresponding rcMRI images.

Discrepancy evaluation at unblinded side-by-side reading

Blinded reading was performed in three patients (four follow-up evaluations) with discrepant radiological tumor status categories. The unblinded side-by-side reading (R1–3) reviewed all examinations (EPIMix and rcMRI) in a collegial discussion aimed to develop a hypothesis by elucidating potential sources of discrepancies between EPIMix and rcMRI. In summary, the unblinded side-by-side reading found no obvious differences in the appearance of the evaluated images between EPIMix and rcMRI, with findings equally discernible in both image sets. However, there was some debate about which lesions were measurable or not, since EPIMix and rcMRI had different slice thicknesses and hence a slight discrepancy in how solid the contrast-enhancing area appeared on imaging, a key criterion in RANO since only solid tumor regions are included in measurements. Detailed results can be found in Supplementary Table 4 and Supplementary Figure 1, 2.

MRI parameters results

Mean (SD) SNR was lower for EPIMix compared to rcMRI on pre-contrast T1-weighted images (18.60 (5.98) vs. 36.88 (15.54), $p< 0.001$, whereas CNR was higher for EPIMix compared to rcMRI (67.81(26.16) vs. 24.70 (11.73)), $p< 0.001$. An adequate mean value signal ghosting of ≤ 0.02 was found for both EPIMix and rcMRI (https://www.acraccreditation.org/-

/media/ACRAccreditation/Documents/MRI/LargePhantomGuidance.pdf). Detailed results for SNR, CNR, and ghosting image artifact values on pre-contrast T1-weighted images are summarized in Supplementary Table 5.

DISCUSSION

This retrospective pilot study aimed to evaluate a new fast brain MRI technique EPIMix compared to rcMRI in adult patients with pathologically confirmed glioma grades 3 and 4 referred for routine MRI follow-ups. Due to its multi-contrast nature, EPIMix demonstrated potential suitability for treatment evaluation in patients with glioma grades 3 and 4.

Among the currently available MRI techniques implemented to shorten MRI scan time, synthetic MRI (9), MRI fingerprinting (8), and rapid-technique MRI (24) have been described. Previously, fast MRI techniques have been evaluated in adult patients with diverse cerebral pathology, suspicion of stroke (25), pediatric patients (26, 27), and patients with brain tumors (28). In a recent study evaluating fast MRI diffusion in brain tumors (28), a strong correlation ρ=0.48 was found between diffusion metrics from fast and conventional protocols. Similarly, in this study comparing a fast with a conventional MRI technique, the fast brain MRI technique EPIMix had almost comparable diagnostic performance to rcMRI at identifying tumor status categories at follow-up. Based on the findings from this study, we hypothesize that the one-minute MRI scan EPIMix could be used as an alternative MRI technique for follow-up of patients with glioma grades 3 and 4 who are unable to undergo a rcMRI examination due to reasons such as discomfort, exhaustion, claustrophobia, restlessness, deteriorated clinical condition, or movement disorders. Further, EPIMix could be used for imaging follow-up in patients at the end of their treatment arsenal when conventional therapies have been exhausted but still deemed to require additional imaging.

A strength of this study is the use of EPIMix in a patient group with a high need for repeated MRI scans during their clinical course. With the availability of repeated scans, there is a potential for closer monitoring of new therapies. The results from this study align with previously published studies investigating EPIMix in different settings and patient groups (10-13). In these previous studies, EPIMix displayed a diagnostic accuracy of ≥ 0.94, a sensitivity of ≥ 0.88, and a specificity of ≥ 0.98 compared to rcMRI (10-12) and did not show evidence of a difference in diagnostic confidence compared to CT ($p \geq 0.10$) (13).

While blinded readers found four cases with discrepant results, the unblinded side-by-side reading correctly identified the tumor status on EPIMix compared to rcMRI in all scans. Divergent measurements of post-contrast T1 area (variability associated with slice position, angulation, or thickness when drawing two perpendicular lines at the slice of maximum tumor diameter) and inter-subject variability in RANO interpretation were hypothesized as potential sources of discrepancies. Based on the results from the unblinded side-by-side reading, we hypothesize that there is a potential for a radiologist to gain even higher diagnostic performance with EPIMix given more training and higher acquaintance with specific method-related artifacts.

Two blinded readers with different levels of experience evaluated EPIMix and rcMRI images following the proposed guidelines for multi-reader studies (29). Despite their varying experience, both readers produced similar results when comparing EPIMix to rcMRI, which enhances the generalizability of the results. SNR mean values on pre-contrast T1-weighted rcMRI were higher than those on EPIMix in absolute values, indicating a higher image quality, although a similar adequate mean value signal ghosting of ≤ 0.02 for image artifacts was found for both methods (https://www.acraccreditation.org/-/media/ACRAccreditation/Documents/MRI/LargePhantomGuidance.pdf).

The specific radiological criteria for MRI evaluation in this study were obtained from the widely used RANO 2.0 criteria for contrast-enhancing gliomas (15). The use of RANO 2.0 criteria ensured a validated scale for tumor status evaluation across readers and enabled an objective comparison of EPIMix and rcMRI.

One study limitation was related to the lack of complete RANO 2.0 evaluation, taking into account leptomeningeal contrast enhancement, clinical status, medication, pseudoprogression, pseudoprogression, and an additional follow-up MRI to confirm the tumor progression. Further, postoperative complications such as abscess or hematoma were not specifically evaluated, nor was pathological tissue confirmation of tumor progression following the radiological assessment. However, since the study aimed to compare two radiological methods performed in the same individual, non-imaging clinical information would not have contributed substantially. Further, leptomeningeal enhancement is a late tumor manifestation in glioma recurrence, often succeeding brain parenchyma tumor progression (30). Another limitation of the study was that the reference standard was based on congruent evaluations by the two blinded readers, potentially leading to observer bias if both were wrong. Further, the small sample size was a result of the limited number of patients with at least two postoperative rcMRI scans and simultaneously acquired EPIMix, and restricted the evaluation of EPIMix at the baso-fronto-temporal regions, prone to present EPI-related image artifacts.

EPIMix does not include 3D T1 pre- and post-contrast images, which are considered standard for imaging surveillance in patients with primary brain tumors and surgical navigation software planning (5), nor does it allow for volumetric tumor measurements. Further, when reading EPIMix, caution must be taken to artifacts near the skull base and metal bone fixations. Despite the unavailability of 3D MRI images, in this study, EPIMix demonstrated high, although slightly lower, diagnostic performance compared to rcMRI for treatment evaluation in patients with glioma grades 3 and 4. A caveat of 3D imaging in motion-prone patients is that artifacts may propagate throughout the whole volume. In such patients, EPIMix may work as a backup or substitute MRI technique due to its inherent motion-robustness.

Finally, as both pre- and post-gadolinium contrast images were acquired, time was lost between scans. To save maximal imaging time, only post-contrast imaging might be considered, especially since EPIMix will also provide T2*-weighted images, which will help to avoid misinterpreting blood products as contrast enhancement.

CONCLUSIONS

In this pilot study, EPIMix was used as a fast MRI alternative for treatment evaluation of patients with glioma grades 3 and 4, with high, but slightly lower diagnostic performance than rcMRI.

ACKNOWLEDGMENTS

The authors would like to thank the statistician Henrike Häbel for her valuable statistical consultation. The authors would also like to thank Dr. Heather Martin for the valuable language consultation. Further, the authors would like to thank the radiographers at the Department of Neuroradiology at Karolinska University Hospital for their assistance in scan acquisition. The authors acknowledge the use of Grammarly (Premium version, https://app.grammarly.com/) for English text editing. The manuscript authors accept full responsibility for the text's factual and citation accuracy, mathematical, logical, and commonsense reasoning, and originality.

REFERENCES

1. Louis DN, Perry A, Wesseling P, Brat DJ, Cree IA, Figarella-Branger D, et al. The 2021 WHO Classification of Tumors of the Central Nervous System: a summary. Neuro Oncol. 2021;23(8):1231-51.
2. Miller KD, Ostrom QT, Kruchko C, Patil N, Tihan T, Cioffi G, et al. Brain and other central nervous system tumor statistics, 2021. CA Cancer J Clin. 2021;71(5):381-406.
3. Weller M, van den Bent M, Preusser M, Le Rhun E, Tonn JC, Minniti G, et al. EANO guidelines on the diagnosis and treatment of diffuse gliomas of adulthood. Nat Rev Clin Oncol. 2021;18(3):170-86.
4. Ellingson BM, Wen PY, Cloughesy TF. Modified Criteria for Radiographic Response Assessment in Glioblastoma Clinical Trials. Neurotherapeutics. 2017;14(2):307-20.
5. Ellingson BM, Bendszus M, Boxerman J, Barboriak D, Erickson BJ, Smits M, et al. Consensus recommendations for a standardized Brain Tumor Imaging Protocol in clinical trials. Neuro Oncol. 2015;17(9):1188-98.
6. Thust SC, Heiland S, Falini A, Jäger HR, Waldman AD, Sundgren PC, et al. Glioma imaging in Europe: A survey of 220 centres and recommendations for best clinical practice. Eur Radiol. 2018;28(8):3306-17.
7. Skare S, Sprenger T, Norbeck O, Rydén H, Blomberg L, Avventi E, et al. A 1-minute full brain MR exam using a multicontrast EPI sequence. Magn Reson Med. 2018;79(6):3045-54.
8. McGivney DF, Boyacıoğlu R, Jiang Y, Poorman ME, Seiberlich N, Gulani V, et al. Magnetic resonance fingerprinting review part 2: Technique and directions. J Magn Reson Imaging. 2020;51(4):993-1007.
9. Tanenbaum LN, Tsiouris AJ, Johnson AN, Naidich TP, DeLano MC, Melhem ER, et al. Synthetic MRI for Clinical Neuroimaging: Results of the Magnetic Resonance Image Compilation (MAGiC) Prospective, Multicenter, Multireader Trial. AJNR Am J Neuroradiol. 2017;38(6):1103-10.
10. Delgado AF, Kits A, Bystam J, Kaijser M, Skorpil M, Sprenger T, et al. Diagnostic performance of a new multicontrast one-minute full brain exam (EPIMix) in neuroradiology: A prospective study. J Magn Reson Imaging. 2019;50(6):1824-33.
11. Kits A, De Luca F, Kolloch J, Müller S, Mazya MV, Skare S, et al. One-Minute Multi-contrast Echo Planar Brain MRI in Ischemic Stroke: A Retrospective Observational Study of Diagnostic Performance. J Magn Reson Imaging. 2021;54(4):1088-95.
12. Af Burén S, Kits A, Lönn L, De Luca F, Sprenger T, Skare S, et al. A 78 Seconds Complete Brain MRI Examination in Ischemic Stroke: A Prospective Cohort Study. J Magn Reson Imaging. 2022;56(3):884-92.
13. De Luca F, Kits A, Martin Muñoz D, Aspelin Å, Kvist O, Österman Y, et al. Elective one-minute full brain multi-contrast MRI versus brain CT in pediatric patients: a prospective feasibility study. BMC Med Imaging. 2024;24(1):23.
14. Bossuyt PM, Reitsma JB, Bruns DE, Gatsonis CA, Glasziou PP, Irwig L, et al. STARD 2015: An Updated List of Essential Items for Reporting Diagnostic Accuracy Studies. Radiology. 2015;277(3):826-32.
15. Wen PY, van den Bent M, Youssef G, Cloughesy TF, Ellingson BM, Weller M, et al. RANO 2.0: Update to the Response Assessment in Neuro-Oncology Criteria for High- and Low-Grade Gliomas in Adults. J Clin Oncol. 2023;41(33):5187-99.
16. Magnotta VA, Friedman L. Measurement of Signal-to-Noise and Contrast-to-Noise in the fBIRN Multicenter Imaging Study. J Digit Imaging. 2006;19(2):140-7.
17. Landis JR, Koch GG. The measurement of observer agreement for categorical data. Biometrics. 1977;33(1):159-74.
18. Mc NQ. Note on the sampling error of the difference between correlated proportions or percentages. Psychometrika. 1947;12(2):153-7.
19. Maxwell AE. Comparing the classification of subjects by two independent judges. Br J Psychiatry. 1970;116(535):651-5.
20. Hanley JA, McNeil BJ. The meaning and use of the area under a receiver operating characteristic (ROC) curve. Radiology. 1982;143(1):29-36.
21. DeLong ER, DeLong DM, Clarke-Pearson DL. Comparing the areas under two or more correlated receiver operating characteristic curves: a nonparametric approach. Biometrics. 1988;44(3):837-45.
22. Rosner B, Glynn RJ, Lee ML. The Wilcoxon signed rank test for paired comparisons of clustered data. Biometrics. 2006;62(1):185-92.
23. Louis DN, Perry A, Reifenberger G, von Deimling A, Figarella-Branger D, Cavenee WK, et al. The 2016 World Health Organization Classification of Tumors of the Central Nervous System: a summary. Acta Neuropathol. 2016;131(6):803-20.
24. Prakkamakul S, Witzel T, Huang S, Boulter D, Borja MJ, Schaefer P, et al. Ultrafast Brain MRI: Clinical Deployment and Comparison to Conventional Brain MRI at 3T. J Neuroimaging. 2016;26(5):503-10.
25. Dhunnoo G, Mukhopadhyay D. Evaluation of the impact of limited-sequence MRI brain protocol (fast brain MRI) on diagnostic accuracy and length of hospital stay for patients with stroke-like symptoms. Clin Med (Lond). 2020;20(Suppl 2):s78-s9.
26. Jaimes C, Yang E, Connaughton P, Robson CD, Robertson RL. Diagnostic equivalency of fast T2 and FLAIR sequences for pediatric brain MRI: a pilot study. Pediatr Radiol. 2020;50(4):550-9.
27. Lindberg DM, Stence NV, Grubenhoff JA, Lewis T, Mirsky DM, Miller AL, et al. Feasibility and Accuracy of Fast MRI Versus CT for Traumatic Brain Injury in Young Children. Pediatrics. 2019;144(4).
28. Loução R, Oros-Peusquens AM, Langen KJ, Ferreira HA, Shah NJ. A Fast Protocol for Multiparametric Characterisation of Diffusion in the Brain and Brain Tumours. Front Oncol. 2021;11:554205.
29. Obuchowski NA, Bullen J. Multireader Diagnostic Accuracy Imaging Studies: Fundamentals of Design and Analysis. Radiology. 2022;303(1):26-34.
30. Andersen BM, Miranda C, Hatzoglou V, DeAngelis LM, Miller AM. Leptomeningeal metastases in glioma: The Memorial Sloan Kettering Cancer Center experience. Neurology. 2019;92(21):e2483-e91.

SUPPLEMENTARY FILES

Supplementary Table 1. STARD checklist *.

Section & Topic	No	Item	Reported on page #
TITLE OR ABSTRACT			
	1	Identification as a study of diagnostic accuracy using at least one measure of accuracy	1, 5-6

		(such as sensitivity, specificity, predictive values, or AUC)	
ABSTRACT			
	2	Structured summary of study design, methods, results, and conclusions (for specific guidance, see STARD for Abstracts)	1
INTRODUCTION			
	3	Scientific and clinical background, including the intended use and clinical role of the index test	1-2
	4	Study objectives and hypotheses	2
METHODS			
Study design	**5**	Whether data collection was planned before the index test and reference standard were performed (prospective study) or after (retrospective study)	2-3
Participants	**6**	Eligibility criteria	2-3
	7	On what basis potentially eligible participants were identified (such as symptoms, results from previous tests, inclusion in registry)	2-3
	8	Where and when potentially eligible participants were identified (setting, location and dates)	2-3
	9	Whether participants formed a consecutive, random or convenience series	2-3
Test methods	**10a**	Index test, in sufficient detail to allow replication	3-5
	10b	Reference standard, in sufficient detail to allow replication	3-5
	11	Rationale for choosing the reference standard (if alternatives exist)	3-5
	12a	Definition of and rationale for test positivity cut-offs or result categories of the index test, distinguishing pre-specified from exploratory	3-5
	12b	Definition of and rationale for test positivity cut-offs or result categories of the reference standard, distinguishing pre-specified from exploratory	3-5
	13a	Whether clinical information and reference standard results were available to the performers/readers of the index test	3-5
	13b	Whether clinical information and index test results were available to the assessors of the reference standard	3-5
Analysis	**14**	Methods for estimating or comparing measures of diagnostic accuracy	4-6
	15	How indeterminate index test or reference standard results were handled	4-6

	16	How missing data on the index test and reference standard were handled	4-6
	17	Any analyses of variability in diagnostic accuracy, distinguishing pre-specified from exploratory	4-6
	18	Intended sample size and how it was determined	10
RESULTS			
Participants	**19**	Flow of participants, using a diagram	3, Figure 1
	20	Baseline demographic and clinical characteristics of participants	6, Table 2
	21a	Distribution of severity of disease in those with the target condition	Table 2
	21b	Distribution of alternative diagnoses in those without the target condition	Table 2
	22	Time interval and any clinical interventions between index test and reference standard	Table 2
Test results	**23**	Cross tabulation of the index test results (or their distribution) by the results of the reference standard	Table 3,4
	24	Estimates of diagnostic accuracy and their precision (such as 95% confidence intervals)	Table 5
	25	Any adverse events from performing the index test or the reference standard	not applicable
DISCUSSION			
	26	Study limitations, including sources of potential bias, statistical uncertainty, and generalisability	9-10
	27	Implications for practice, including the intended use and clinical role of the index test	9-10
OTHER INFORMATION			
	28	Registration number and name of registry	3
	29	Where the full study protocol can be accessed	2-6
	30	Sources of funding and other support; role of funders	Funding section

*17. Bossuyt PM, Reitsma JB, Bruns DE, Gatsonis CA, Glasziou PP, Irwig L, et al. STARD 2015: An Updated List of Essential Items for Reporting Diagnostic Accuracy Studies. Radiology. 2015;277(3):826-3

Supplementary Text 1. Patients' search strategy.

% 1. multiex in risdata.

SELECT PatientID, COUNT(PatientID) FROM risdata WHERE Modality = "MR" AND AccessionNumber =

EPIMixAccessionNumber GROUP BY PatientID HAVING COUNT(PatientID) > 1

%2. hgg with StudyRadReport, ReqQuestion and ReqAnamnesis

CREATE VIEW hgg AS (SELECT * FROM risdata WHERE Modality = "MR" AND

(lower(StudyRadReport) LIKE "%lioblastom%" OR lower(ReqQuestion) LIKE "%lioblastom%" OR lower(ReqAnamnesis) LIKE "%lioblastom%") OR

(lower(StudyRadReport) LIKE "%höggrad%" AND lower(StudyRadReport) LIKE "%tumör%") OR

(lower(StudyRadReport) LIKE "%anaplastisk%" AND (lower(StudyRadReport) LIKE "%cytom%" OR lower(StudyRadReport) LIKE "%ligodendrogliom%" OR lower(StudyRadReport) LIKE "%pendymo%")) OR (lower(ReqQuestion) LIKE "%anaplastisk%" AND

(lower(ReqQuestion) LIKE "%cytom%" OR lower(ReqQuestion) LIKE "%ligodendrogliom%" OR lower(ReqQuestion) LIKE "%pendymo%"))

OR (lower(ReqAnamnesis) LIKE "%anaplastisk%" AND

(lower(ReqAnamnesis) LIKE "%cytom%" OR lower(ReqAnamnesis) LIKE "%ligodendrogliom%" OR lower(ReqAnamnesis) LIKE "%pendymo%")))

%3. hgg and multiex exams

CREATE VIEW hgg_multiex AS (SELECT M.PatientID FROM multiex AS M INNER JOIN hgg AS T ON M.PatientID = T.PatientID)

%4 risdata info for hgg_multiex

CREATE VIEW risdata_hgg_multiex AS

(SELECT

R.EPIMixAccessionNumber,R.PatientID,R.StudyRadReport,R.ReqQuestion,R.ReqAnamnesis,R.DateAcquired,R.StudyDescription

FROM risdata AS R INNER JOIN hgg_multiex AS T ON R.PatientID = T.PatientID WHERE R.Modality = "MR")

%5 risdata info for hgg_multiex, both AccessionNumber and EPIMixAccessionNumber

CREATE VIEW risdata_hgg_multiex_acc AS

(SELECT R.AccessionNumber,

R.EPIMixAccessionNumber,R.PatientID,R.StudyRadReport,R.ReqQuestion,R.ReqAnamnesis,R.DateAcquired,R.StudyDescription

FROM risdata AS R INNER JOIN hgg_multiex AS T ON R.PatientID = T.PatientID WHERE R.Modality = "MR")

%6 risdata_hgg_multiex and coupled countID >1 n56

CREATE VIEW risdata_hggmultiex_countid AS (SELECT PatientID, COUNT(PatientID) FROM risdata_hgg_multiex_acc WHERE AccessionNumber = EPIMixAccessionNumber GROUP BY PatientID HAVING COUNT(PatientID) > 1)

%7 FIND patients in hgg_multiex that are not in risdata_hggmultiex_countid

CREATE VIEW backup AS (SELECT * FROM hgg_multiex WHERE NOT EXISTS (SELECT * FROM risdata_hggmultiex_countid WHERE risdata_hggmultiex_countid.PatientID = hgg_multiex.PatientID))

Supplementary Table 2. Detailed information on routine clinical MRI (rcMRI) scan protocols.

Protocol 1.5 T

Scan time (min:s)	Sequence	Scan plane	Slice thickness (mm)
00:17	**0. Scout**	3 plane	-
04:45	**1. 3D T2 FLAIR CUBE #**	Sagittal	1.4
01:51	**2. DWI**	Axial	4
02:48	**3. SWI 3D ##**	Axial	2
03:50	**4. 3D T1 GRE IR BRAVO**	Axial	1.2
01:27	**5. DSC Perfusion + Gd***	Axial	4
03:26	**6. T2 PROPELLER + Gd**	Axial	4
03:50	**7. 3D GRE IR BRAVO + Gd**	Axial	1.2
02:32	**8. T1 FLAIR PROPELLER + Gd***	Axial	4

Gd = Intravenous gadolinium contrast
DSC= Dynamic susceptibility contrast
# Until December 2018, instead of 3D T2 FLAIR Cube, 2D T2 FLAIR was occasionally used (axial or coronal, 4 mm, 03:36)
# # Until December 2018, instead of 3D SWI, T2* EPI was used (axial, 4mm, 00:27). In-house 3D SWI EPI sequence developed at Karolinska University Hospital.
*Additional sequence, on a specific request of the neuroradiologist
Total image acquisition time = scan time 20:47 (min:s) without additional sequence and without prescan time, download time, and extra slice planning time.

Protocol 3T			
Scan time (min:s)	**Sequence**	**Scan plane**	**Slice thickness (mm)**
00:33	**0. Scout**	3 plane	-
04:08	**1. 3D T2 FLAIR CUBE**	Sagittal	1.2
02:20	**2. DWI**	Axial	4
02:24	**3. SWI 3D #**	Axial	2
03:50	**4. 3D T1 GRE IR BRAVO**	Axial	1.4
01:27	**5. DSC Perfusion + Gd***	Axial	4
02:40	**6. T2 PROPELLER + Gd**	Axial	4
03:50	**7. 3D GRE IR BRAVO + Gd**	Axial	1.4
02:32	**8. T1 FLAIR PROPELLER + Gd***	Axial	4

Gd = Intravenous gadolinium contrast
DSC= Dynamic susceptibility contrast
# Until December 2018, instead of 3D SWI, T2* EPI was used (axial, 4mm, 00:38). In-house 3D SWI EPI sequence developed at Karolinska University Hospital.
*Additional sequence, on a specific request of the neuroradiologist
Total Image acquisition time = scan time 19:45 without additional sequence and without prescan time, download time, and extra slice planning time.

Supplementary Text 2. Detailed instructions for radiological assessment of high-grade glioma modified from RANO criteria*.

- Identification of pseudo-enhancing lesions when lesions were high-signaling on both non-contrast and contrast T1-weighted images.

- Identification of true contrast-enhancing lesions when lesions presented as low-signaling on non-contrast T1w and high-signaling on contrast T1w. True contrast-enhancing lesions were further classified as measurable and nonmeasurable. Measurable lesions were identified when meeting all of the following criteria:

    - Contrast-enhancing lesions with clearly defined margins

- Contrast-enhancing tumor area obtained by multiplying two maximal perpendicular diameters of at least 10 mm in size and visible on two or more axial slices (slice thickness <5 mm)
- Exclusion of cystic cavities from the measurement of the tumor area.

* Wen PY, van den Bent M, Youssef G, Cloughesy TF, Ellingson BM, Weller M, et al. RANO 2.0: Update to the Response Assessment in Neuro-Oncology Criteria for High- and Low-Grade Gliomas in Adults. J Clin Oncol. 2023;41(33):5187-99.

Supplementary Table 3. Weighted Cohen's kappa interpretation.

Weighted Cohen's kappa	κ
Slight agreement	0.00-0.20
Fair agreement	0.21-0.40
Moderate agreement	0.41-0.60
Substantial agreement	0.61-0.80
Almost perfect agreement	0.81-1.00

Supplementary Table 4. R1-2 blinded reading (EPIMix, rcMRI) and R1-3 unblinded side-by-side reading (EPIMix, rcMRI).

ID	Brain tumor follow-up evaluation	R1 EPIMix	R2 EPIMix	R1 rcMRI	R2 rcMRI	R1-3 Unblinded side-by-side reading comments
9	Baseline vs. 1st follow-up scan	SD	SD	SD	PD	Progression of a contrast-enhancing lesion from being non-measurable at baseline to measurable at 1st follow-up on both EPIMix and rcMRI. Tumor status category determined to be PD.
9	Baseline vs. 2nd follow-up scan	SD	SD	SD	PD	Stable CE lesion between baseline and 2nd follow-up, equally visible and nonmeasurable on both EPIMix and rcMRI. Tumor status category determined to be SD.
12	Baseline vs. 1st follow-up scan	PD	PD	SD	SD	Stable CE lesion between baseline and follow-up, equally visible on both EPIMix and cMRI. Tumor status category determined to be SD.
26	Baseline vs. 1st follow-up scan	SD	PR	SD	PR	Stable CE lesion between baseline and follow-up, equally visible and measurable on both EPIMix and cMRI. Tumor status category determined to be SD.

In detail:

- ID 9, baseline vs. 1st follow-up, was evaluated as SD on EPIMix R1–2 and rcMRI R1, whereas PD on rcMRI R2 on blinded reading. However, unblinded side-by-side reading determined the contrast-enhancing lesion as progressing from "nonmeasurable" at baseline to "measurable" on the 1st follow-up scan on both EPIMix and rcMRI, and hence categorized as PD.
- ID 9, baseline vs. 2nd follow-up, evaluated at blinded reading as PD on rcMRI R2, but SD on EPIMix R1–2 and rcMRI R1. The unblinded side-by-side reading determined the contrast-enhancing lesion as "nonmeasurable" on the 2nd follow-up scan compared to baseline on both EPIMix and rcMRI, and hence categorized as SD.
- ID12, baseline vs. 1st follow-up, was evaluated at blinded reading as PD on EPIMix R1–2, whereas SD on rcMRI R1–2. The unblinded side-by-side reading determined the contrast-enhancing lesion as being "nonmeasurable" on the 1st follow-up scan compared to baseline on both EPIMix and rcMRI, and hence categorized as SD.

- ID26, ID 9, baseline vs. 1st follow-up, was evaluated at blinded reading as PR on EPIMixR2 and rcMRIR2, but SD on EPIMixR1 and rcMRIR1. The unblinded, side-by-side reading determined the measurable contrast-enhancing lesion as stable on the 1st follow-up scan compared to baseline on both EPIMix and rcMRI, and hence categorized as SD.

Supplementary Figure 1. ID 9. T1-, T1 post-contrast images. Baseline (A), first follow-up (B), and second follow-up (C). EPIMix (left), rcMRI (right). Measurements of the contrast-enhancing lesions as per unblinded side-by-side consensus reading are displayed on the images. Detailed information about the visual discrepancies and evaluation from the unblinded side-by-side consensus reading are provided in Supplemental file 5.

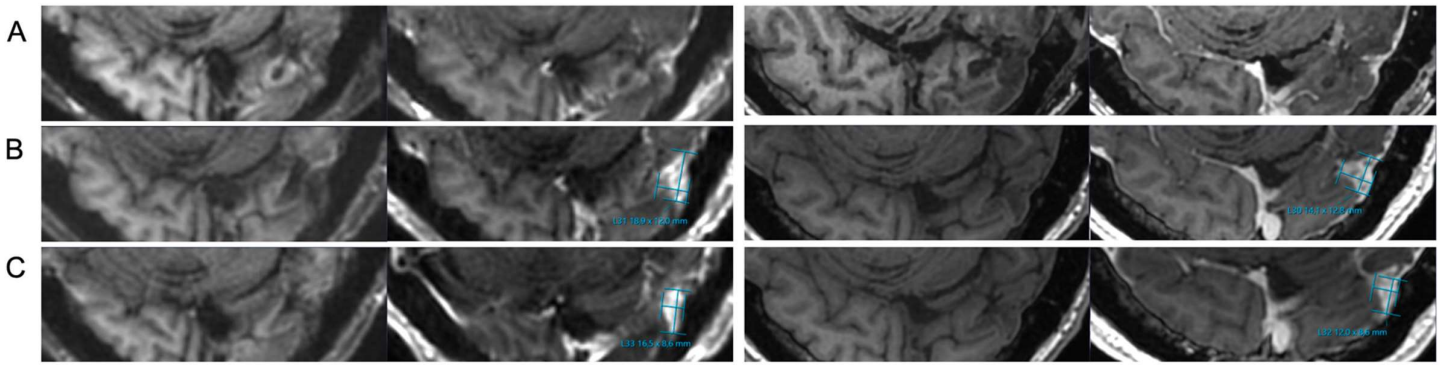

Supplementary Figure 2. ID 12. T1-, T1 post-contrast images. A and B, EPIMix baseline and follow-up; C and D, rcMRI baseline and follow-up. Stable contrast-enhancing lesion on both EPIMix and cMRI (arrow).

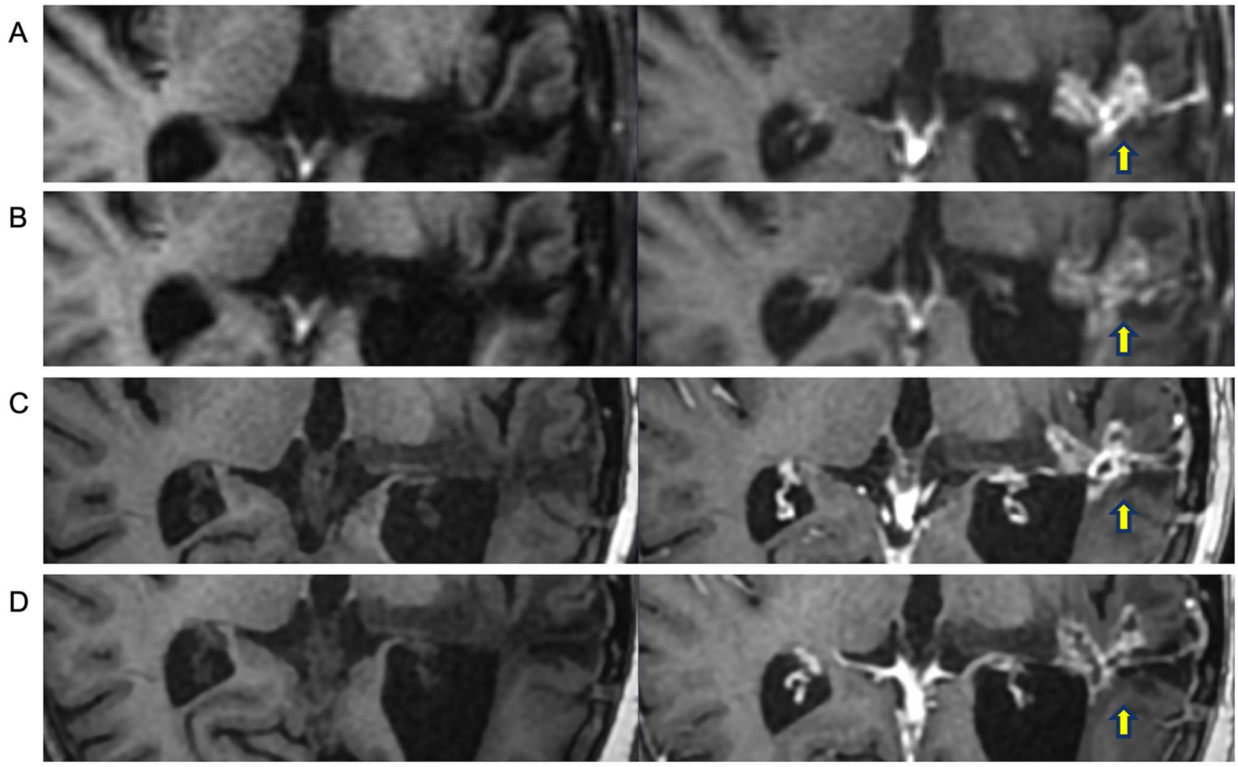

Supplementary Table 5. Signal-to-noise (SNR), contrast-to-noise (CNR), ghosting image artifacts mean values, standard deviation (SD), and range for EPIMix and rcMRI on pre-contrast T1-weighted images.

mean, SD (range)	SNR	CNR	Ghosting Image artifacts
EPIMix	18.60, 5.98 (7.44–39.78)[a]	67.81, 26.16 (4.36–115.16)[a]	0.01, 0.01 (0–0.07)[c]
rcMRI	36.88, 15.54 (8.01–88.33)[b]	24.70, 11.73 (1.27–53.78)[b]	0.02, 0.02 (0–0.20)[d]

[a] 3/93 exams were not evaluated on EPIMix, out of which in one case due to the unavailability of pre-contrast T1 weighted image and in two other cases due to the impossibility of retrieving the pre-contrast T1 weighted images in the local database.
[b] 1/93 exams were not evaluated on rcMRI due to the unavailability of the axial pre-contrast T1 weighted image.
[c] 10/93 exams were not evaluated on EPIMix, in one case due to unavailability of pre-contrast T1 weighted image, in two other cases due to the impossibility of retrieving the pre-contrast T1 weighted images in the local database, in the remnant cases due to insufficient field of view for the calculation of the top and/or bottom ROI.
[d] 9/93 exams not evaluated on rcMRI, in one case due to unavailability of axial pre-contrast T1 weighted image, in the other eight cases due to insufficient field of view for the calculation of the top and/or bottom ROI.